Exploring the link between cation exchange capacity and magnetic susceptibility

Gaston Matias Mendoza Veirana[1], Hana Grison[2], Jeroen Verhegge[1,3], Wim Cornelis[1], Philippe De Smedt[1,3]

[1]Department of Environment, Faculty of Bioscience Engineering, Ghent University, Coupure Links 653, geb. B, 9000 Ghent, Belgium.
[2] Institute of Geophysics of the Czech Academy of Sciences, Boční II/ 1401, 14100 Prague 4, Czech Republic
[3] Department of Archaeology, Ghent University, Sint-Pietersnieuwstraat 35-UFO, 9000 Ghent, Belgium.

Correspondence to: Gaston Matias Mendoza Veirana (Gaston.MendozaVeirana@ugent.be)

Abstract. This study explores the relationship between soil magnetic susceptibility (κ) and cation exchange capacity (CEC) across diverse European soils, aiming to enhance pedotransfer functions (PTFs) for soil CEC using near-surface electromagnetic geophysics. We hypothesize that soil κ, can improve the prediction of CEC by reflecting the soil's mineralogical composition, particularly in sandy soils.

We collected data from 49 soil samples in vertical profiles across Belgium, the Netherlands, and Serbia, including κ in field conditions (κ^*), low and high frequency κ in the laboratory, in-site electrical conductivity (σ), iron content, soil texture, humus content, bulk density, water content, water pH, and CEC. We used these properties as features to develop univariable and multivariable (in pairs) polynomial regressions to predict CEC for sandy and clayey soils.

Results indicate that κ^* significantly improves CEC predictions in sandy soils, independent of clay content, with a combined κ^*-σ model achieving the highest predictive performance ($R^2 = 0.94$). In contrast, laboratory-measured κ was less effective, likely due to sample disturbance.

This study presents a novel CEC PTF based on σ and κ^*, offering a rapid, cost-effective method for estimating CEC in field conditions. While our findings underscore the value of integrating geophysical measurements into soil characterization, further research is needed to refine the κ-CEC relationship and develop a more widely applicable model.

1 Introduction

Modern strategies for soil characterization are crucial for addressing the global challenges of soil degradation and pollution. Near-surface electromagnetic geophysics, in particular, facilitates rapid quantitative assessment of soils, offering insights

into subsurface electrical conductivity (σ), dielectric permittivity (ε), and magnetic susceptibility (κ) (Garré et al., 2022; Romero-Ruiz et al., 2018). Data collected on these electromagnetic properties can be used for direct qualitative soil survey interpretations or for more comprehensive quantitative analyses involving pedophysical models and pedotransfer functions.

Pedophysical models (PMs) link depth-specific geophysical properties with common soil properties. The need for developing such models is growing due to the demand for high-precision soil characterization (Romero-Ruiz et al., 2018; Verhegge et al., 2021; Wunderlich et al., 2013). Pedotransfer functions (PTFs) are models used to predict soil properties that are typically costly to obtain and are therefore determined less frequently than soil attributes that can be characterized more effectively (Van Looy et al., 2017).

An important indicator of soil health and fertility, which is also crucial in most PMs and PTFs, is the cation exchange capacity (CEC) (Glover, 2015; Mendoza Veirana et al., 2023). Defined as the ability of a soil to hold and exchange cations (Khaledian et al., 2017), CEC is highly correlated with the soil clay content due to a larger colloid surface for particle exchanges. Furthermore, as it is influenced by the soil's physical (e.g., texture), chemical (e.g., pH, mineralogy), and biological properties (e.g., organic matter), CEC integrates aspects from all three main indicator groups commonly used to assess soil quality (Khaledian et al., 2017). Several PMs for soil σ prediction include CEC due to the significant influence of free charges on σ, despite the contribution of other properties such as water content (θ) and salinity or bulk soil σ (Glover, 2015). Soil charges can be either permanent or variable, depending primarily on soil pH (Chapman, 1965; Sumner & Miller, 2018). The relationship between clay content and CEC can be highly variable due to its dependence on clay mineralogy (ranging from 3-15 meq/100g for kaolinite to 100-150 meq/100g for vermiculite), and the relative proportion of variable and permanent CEC varies among clay minerals (Miller, 1970; Seybold et al., 2005). To standardize CEC measurements under varying soil conditions, it is common to use the CEC in neutral pH conditions (=7) $CEC7$. However, conventional analytical methods for measuring CEC, such as the sodium saturation method, are time-consuming and expensive (Busenberg & Clemency, 1973). Due to the critical importance of CEC, its measurement cost, and its correlation with other soil properties, numerous PTFs (Khaledian et al., 2017) and worldwide hybrid models (Poggio et al., 2021) for $CEC7$ have been developed. Commonly, CEC PTFs are expressed in function of clay content and humus, and less frequently pH and soil depth (Khaledian et al., 2017; Seybold et al., 2005). While commonly CEC PTFs are multivariate polynomial regressions, machine learning methods are used in the last decade when large datasets are available, as artificial neural networks (Ghorbani et al., 2015), and genetic expression programming and multivariate adaptive regression splines (Emamgolizadeh et al., 2015). However, when working with small datasets, polynomial regressions are often preferred. Additionally, results have shown that σ and soil magnetic susceptibility (κ) are independent (Maier et al., 2006), even though they generally correlate well with CEC.

Soil magnetic susceptibility has been correlated positively with CEC in studies focusing on soil type identification (de Mello et al., 2020), soil characterization (Siqueira et al., 2010), paleoclimatic reconstruction (Maher, 1998), and electromagnetic

induction applications (McLachlan et al., 2022). κ describes a material's ability to become magnetized when subjected to an external magnetic field. It quantifies the degree of magnetization induced in the substance relative to the strength of the applied magnetic field. Formally, κ is defined as $\kappa = H/M$, where M is the induced magnetization of the material and H is the applied magnetic field. Soil κ measurements are widely used to detect the presence of pedogenic ferrimagnetic minerals (Dearing et al., 1996). The composition of the source material, and consequently the mineralogy of the rocks and sediments that formed the soils, are the main parameters influencing soil magnetic properties (Jordanova, 2017).

Soil clay content and soil κ are correlated positively due to the presence of ferrimagnetic minerals (such as maghemite) in the clay fraction, originating either from the source material or through pedogenesis (de Mello et al., 2020). Consequently, it has been suggested that the observed correlation between κ and CEC is actually due to their mutual correlation with clay content, indicating that there may not be a direct effect of κ on CEC (de Mello et al., 2020).

To the best of our knowledge, the κ-CEC relationship has not been studied beyond the site level (Siqueira et al., 2010). This leaves any physicochemical mechanism that might link the permanent component of CEC and soil κ unexplored.

The main hypothesis is that soil κ can support characterizing soil mineralogy, which also influences the permanent component of CEC. Therefore soil κ may significantly enhance the accuracy of CEC PTFs, which can help evaluating field CEC rapidly, and at low cost. To improve predictions of field CEC by integrating soil κ we develop and test uni- and multivariate polynomial PTFs based on data of diverse soil types sampled in Europe. In addition, we explore soil κ measured in-situ and in laboratory at different frequencies to give insights into the κ-CEC relationship and investigate how clay content affects the relationship between κ and CEC.

To ensure transparency and reproducibility, all the collected data and developed code for this work is publicly available in (Mendoza Veirana, 2024).

2 Methods

2.1 Study area, field measurements, and soil analysis

From 8 sites in Belgium, the Netherlands and Serbia, 49 soil samples were collected across a wide range of USDA soil textures from sand to clay, and WRB soil types (Figure 1 and Table 1, see also Mendoza Veirana et al. (2023)), At each site, test pits were dug to identify and sample different soil horizons. For each soil horizon and within a vertical soil profile, soil field κ was measured (κ_*) (5 to 11 measurements per site, 49 in total) using a kappa meter SM30 (ZH Instruments, Brno, Czech Republic) at 8 kHz. The sensor measures soil κ with a penetration depth of 2 cm and a sensitivity of 10^{-7} SI units. First, the sensor was placed against the soil's profile wall for a measurement, followed by an additional measurement taken in open air away from the profile to obtain a reference zero κ value for measurement calibration (ZH instruments, 2022).

90   Additionally, a HydraProbe sensor (Stevens, Water Monitoring Systems) was employed to measure σ along the profile wall. The correction proposed by Logsdon et al. (2010) was applied to improve the quality of these readings.

Undisturbed soil samples of 100 cm³ were collected by manually pushing standard steel rings horizontally into the soil profile wall at the same locations where κ_* was measured. These samples were used to determine volumetric water content (θ) and bulk density (b_d) after drying them for 24 hours at 105 °C (Grossman and Reinsch, 2002).

95   Disturbed soil samples of about 250 g were collected around the undisturbed samples. They were air-dried, homogenized in an agate mortar, and sieved using a 2 mm mesh for determination of texture, and chemical and magnetic soil properties. Clay, silt and sand content (denoted as Clay, Silt, Sand, respectively, expressed in %) was measured following ISO 11464, content of humus, CEC was determined by CoHex (Ciesielski et al., 1997a, 1997b).

100

	Samples	Soil type	Depth [cm]	*Sand* [%]	*Clay* [%]	κ_* [10^{-5}]	κ_{lf} [10^{-5}]	κ_{fd} [-]	*Fe* [ppm]	*Humus* [%]	σ [mS/m]	*CEC* [meq/ 100g]
A	5	Luvisols	[4,106]	[9,16]	[9,13]	[14,32]	[14,40]	[5.2,8.1]	[14,21]	[0.1,2.3]	[12,35]	[6,9]
DREN	5		[72,252]	[18,35]	[27,39]	[47,66]	[51,70]	[6.2,9.1]	[31,38]	[0.6,1.6]	[30,53]	[20,25]
E	5	Cambisols	[20,110]	[24,35]	[20,25]	[7.2,14]	[8,15]	[3.5,5.5]	[19,25]	[0.8,2.6]	[38,50]	[9,12]
EH2	5	Phaeozems	[20,94]	[10,54]	[17,53]	[12,20]	[13,38]	[3.2,6.7]	[42,50]	[0.3,5.7]	[55,66]	[16,39]
HOEKE	11	Cambisols	[28,258]	[9,45]	[16,32]	[4.5,116]	[6.8,127]	[4.4,8.1]	[17,34]	[0.5,11]	[27,59]	[8,30]
P	7	Retisols	[32,144]	[42,80]	[8,11]	[2.6,12]	[4.5,16]	[2.9,8.5]	[5.9,12]	[0,2]	[8,17]	[1.6,11]
S	5	Arenosols	[28,130]	[83,93]	[5,7]	[3,20]	[2.9,73]	[3.3,9.2]	[3.6,16]	[0,2]	[11,29]	[2,5]
VALTHE	6	Podzol	[10,60]	[91,95]	[3,4]	[0.8,12]	[1.2,19]	[3.9,9.7]	[1,2.5]	[0,2.2]	[0.5,1]	[1.6]
All	49		[4,252]	[9,95]	[3,53]	[0.8,116]	[1.2,127]	[2.9,9.7]	[1,50]	[0,11]	[0,66]	[1.6,39]

Table 1 Minimum and maximum intervals of soil and magnetic properties for each explored site. Data ranges reflect the diversity of soil types and conditions across various sites.
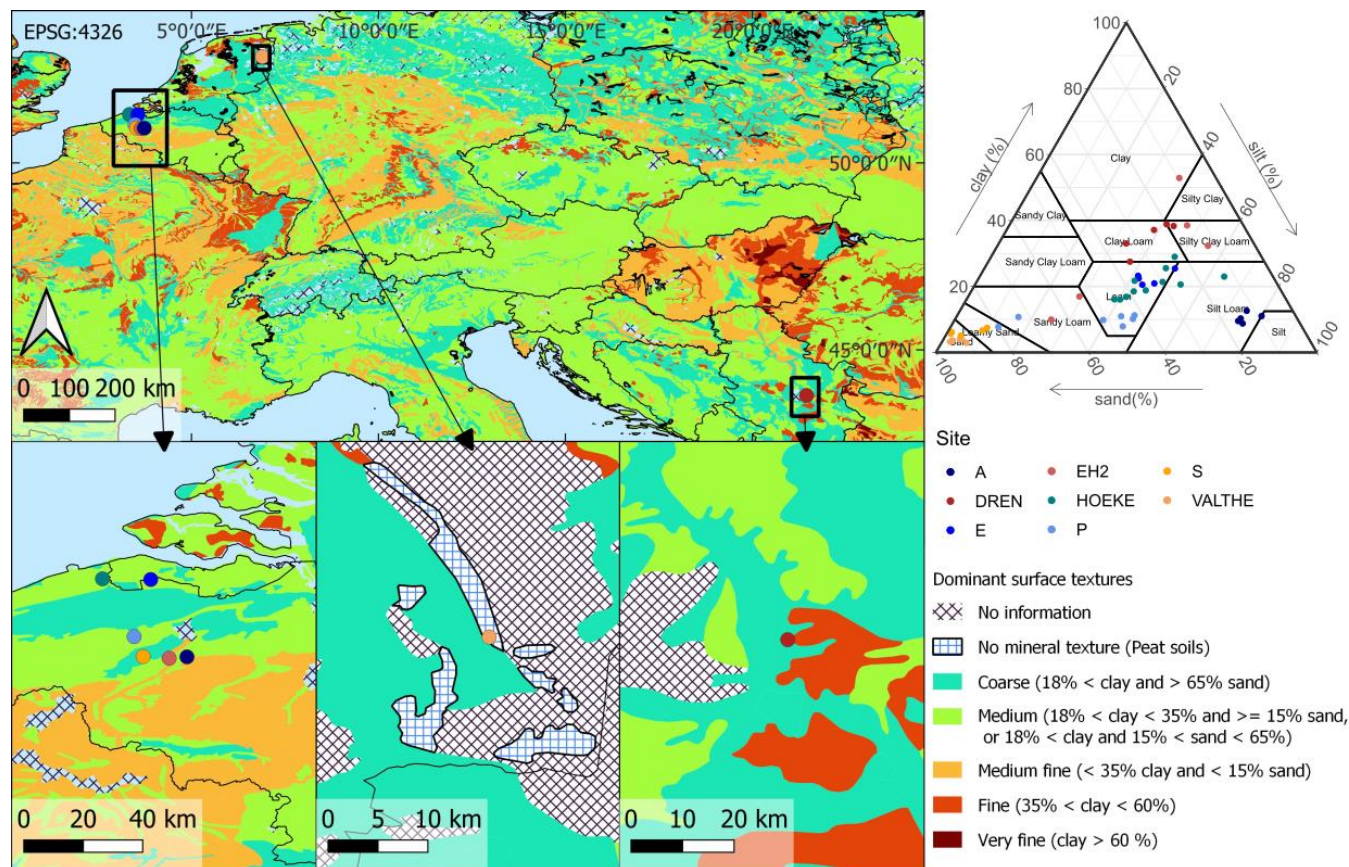
Figure 1 Locations of the study sites. Background shows dominant surface texture (European Soil Database v2.0, 2004). Colors represent the texture of the sites: sandy in yellowish, silty in blueish and clayey in reddish. USDA texture triangle showing the particle size distribution categorized by sampling site. The samples presented in Table 1 are represented by triangles (adapted from (Mendoza Veirana et al., 2023)).

Magnetic susceptibility κ was measured using a Kappabridge MKF1-FA (AGICO Instruments, Brno, CZ), in addition to the field κ measurements. Prior to these laboratory measurements, corrections were made to eliminate the influence of the diamagnetic sample holder. Samples were placed in 10 cm³ plastic holders, and the in-phase κ was recorded at both low frequency (κ_{lf}) and high frequency (κ_{hf}) (976 Hz and 15616 Hz, respectively). Thus, the percentage frequency dependent magnetic susceptibility (κ_{fd}) was calculated as:

$$\kappa_{fd} = \frac{\kappa_{lf} - \kappa_{hf}}{\kappa_{lf}} \times 100 \ [\%]$$

Equation 1

115 Additionally, the absolute difference ($\kappa_{fd\ abs} = \kappa_{lf} - \kappa_{hf}$) was calculated. Such measurements are used to detect the presence of superparamagnetic ferrimagnetic minerals occurring as ultrafine (<0.03 μm) crystals produced largely by pedogenic biochemical processes in soil (Dearing, 1994). Samples where ultrafine minerals are present will show increased frequency dependent magnetic susceptibility; samples without such minerals will show identical κ values at the two frequencies.

120 To support magnetic observations, elemental analyses were performed to evaluate the total iron content concentration (Fe) of all samples through X-ray fluorescence (XRF, Niton XL3t GOLDD+, Thermo Fisher Scientific Inc., USA) on samples that passed a 0.5 mm sieve and placed in capsules covered with 4^{-6} m cellophane. Three consecutive XRF measurements were performed and averaged for each sample.

2.2 Model development

125 Developing a CEC PTF using soil κ data that can be generalized beyond site-specific is a challenging task, requiring careful consideration of the data used for model development. The absence of previous attempts at this highlights the importance of thorough data exploration. We chose to build polynomial models due to their interpretability, simplicity, and the use of only one tuning parameter (polynomial degree), which is suitable given the relatively small dataset (n=49).

130 Field and laboratory measured soil properties were used as features for predicting CEC (target variable), these are: soil depth, water pH, $Humus$, $Clay$, $Silt$, and $Sand$, b_d, σ, κ_*, κ_{lf}, κ_{fd}, $\kappa_{fd\ abs}$, and Fe. All (13) features were used to develop univariable polynomial regressions, and multivariable models were created by combining features in pairs, resulting in 91 feature combinations. The top four combinations in terms of test performance were compared to the standard combination of $Clay$ and $Humus$ content, also, single features were considered ($Clay$, σ, and κ_*).

135 Since model performance was largely dependent on clay content, the samples were divided into sandy (n=25) and clayey (n=24) groups, using the median clay content (16.1%) as a threshold. Both input datasets were split randomly into training (70%) and testing (30%) subsets, without consideration of any soil characteristics. This approach ensured that samples from different sites, soil horizons, and physicochemical properties were mixed during data splitting. To further ensure an unbiased model evaluation, the training and testing process was repeated 100 times. The best polynomial degree (linear or quadratic)

140 was determined by the highest median of the R^2 test scores over the 100 repetitions. Finally, model implementation was performed after tuning and feature selection using all the samples of each subset.

2.3 Statistical analysis

Predicting CEC based on soil properties, particularly focusing on magnetic characteristics is a multivariate problem.

145 Commonly, many variables are linearly correlated with CEC, such as $Clay$, κ, Fe, $Humus$, and σ. The challenge lies in

distinguishing between independent and masked effects. Importantly, the positive correlation between κ and CEC may be due to the strong correlation between clay content and both CEC and κ (de Mello et al., 2020).

To address this, we quantified the independent correlation between κ and CEC, irrespective of the effects of clay by calculating the partial correlation, that is the correlation between the residuals of the linear fitting of the covariable (*Clay*)

150 with the variables (κ and CEC).

3 Results and discussion

3.1 Data exploration

155 A general variable exploration analysis is presented in this section, which is fundamental for the model development in the next section. Spearman's rank correlations between all the features mentioned and target can be seen in Figure 2. As expected, soil κ is less correlated to CEC than common soil properties such as *Clay* and *Sand*, water pH and θ, while *Fe* and σ correlate strongly with CEC. Additionally, consistent with the findings of de Mello et al. (2020) and Ayoubi et al. (2018), there is a positive correlation between *Clay* and κ (both κ_* and κ_{lf}). Also in line with Maier et al. (2006), σ is not correlated

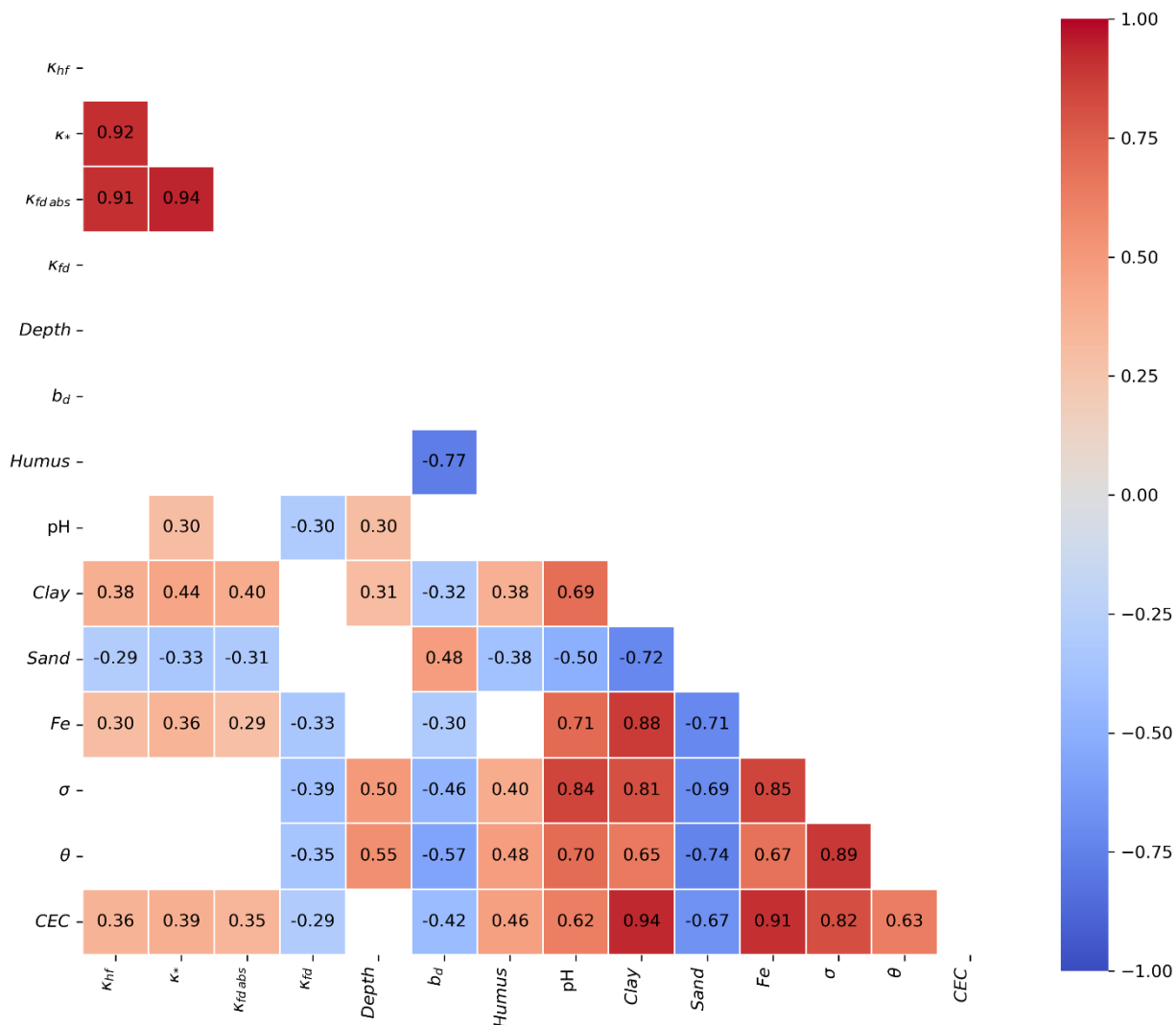160 significantly to κ. Conversely, *Sand* correlates negatively with both κ and *Fe*.

Figure 2 Spearman rank correlation heatmap showing significant P-values<0.005 for the 49 soil samples.

165   Comparing soil κ_* to κ_{lf} reveals a similar trend across the entire range of observations (10^{-5} to 10^{-3}) (see Figure 3). This trend persists despite κ_* being measured in undisturbed soil structures with field bulk density, while κ_{lf} was obtained from repacked samples that do not preserve the field structure and density. Additionally, the measurement frequency for κ_* (8 kHz) differs from that of κ_{lf} (~1 kHz).

9
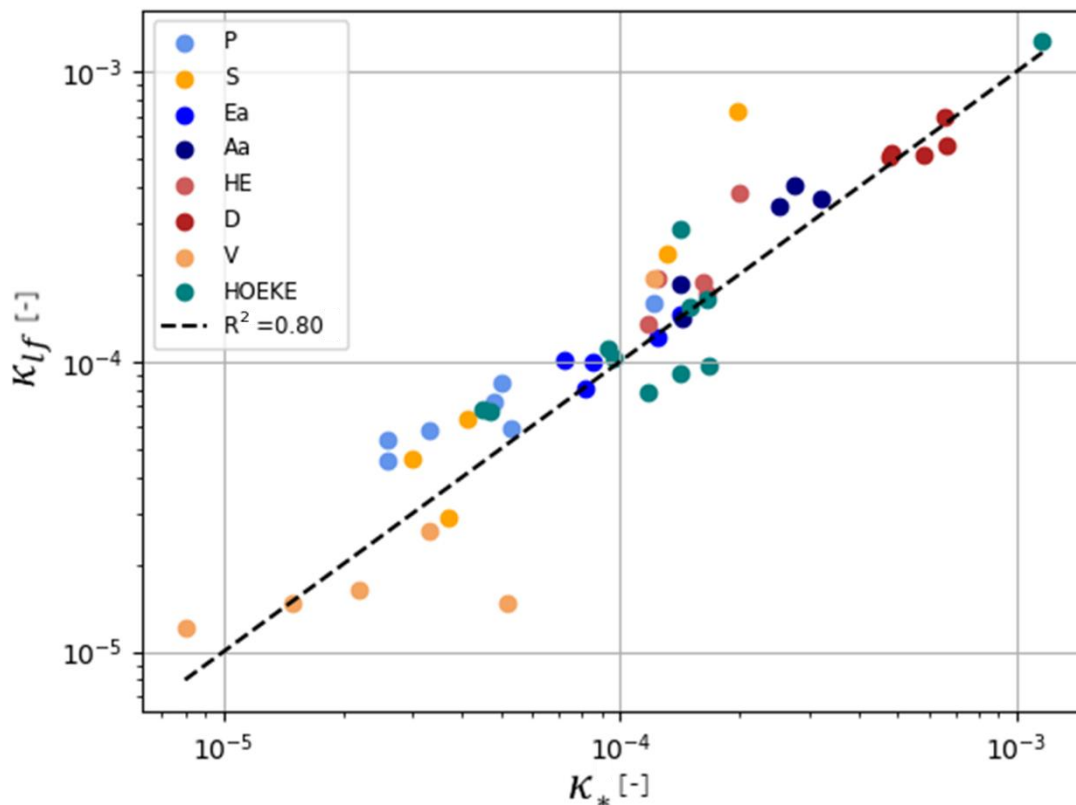
Figure 3 Logarithmic scatter plot showing the field observed magnetic susceptibility vs the laboratory observed low frequency magnetic susceptibility.

3.2 *CEC* modelling

Model training and testing was performed in sandy and clayey groups independently. The predictors for CEC, with the best overall model performance, turned out to be highly dependent on the group. Notably, using σ and κ_* provided the best prediction results on the sandy group, with training and testing median R^2 values of 0.95 and 0.85, respectively (see Figure 4). This performance is significantly higher than that achieved with the commonly used features, such as *Clay* and *Humus* content, which had a median test R^2=0.38. Additionally, the combination of *Sand* and *pH* performed equally well, followed closely by combinations of κ_* and κ_{lf} features.
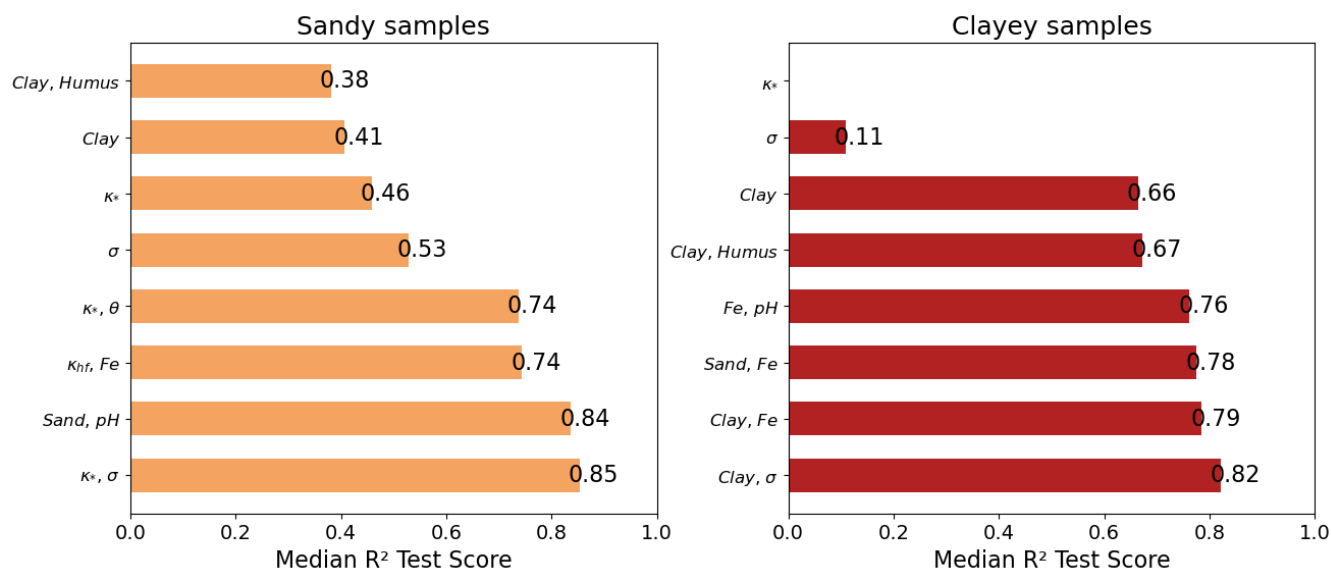
10

Figure 4 Horizontal bar plot showing test model performances of CEC prediction based on different features (vertical axis) for sandy and clayey samples. Features shown here are the top four in performance (bottom), and κ_*, σ, Clay, and the pair Clay, Humus.

The strong performance of σ and κ_* as predictor of CEC in sandy soils can be explained by the variable nature of σ as it depends on state variables, as well as the variable component of CEC. The strong predictive capacity of κ_* likely captures the permanent component of CEC, which in sandy soil is mainly linked to soil mineralogy due to low colloid surface. Additionally, both σ and κ_* can be quickly measured in field conditions without the need for invasive sampling. Therefore, after implementing the best CEC PTF for sandy samples (see Figure 5):

$$CEC = 1.233 + 14000 \cdot \kappa_* - 0.00861 \cdot \sigma - 5.91 \cdot 10^7 \cdot \kappa_*{}^2 + 1350 \cdot \kappa_* \cdot \sigma + 0.000624 \cdot \sigma^2; R^2 = 0.94$$

Equation 2

Where κ_* is unitless, σ is in mS/m and CEC in meq/100g .

11
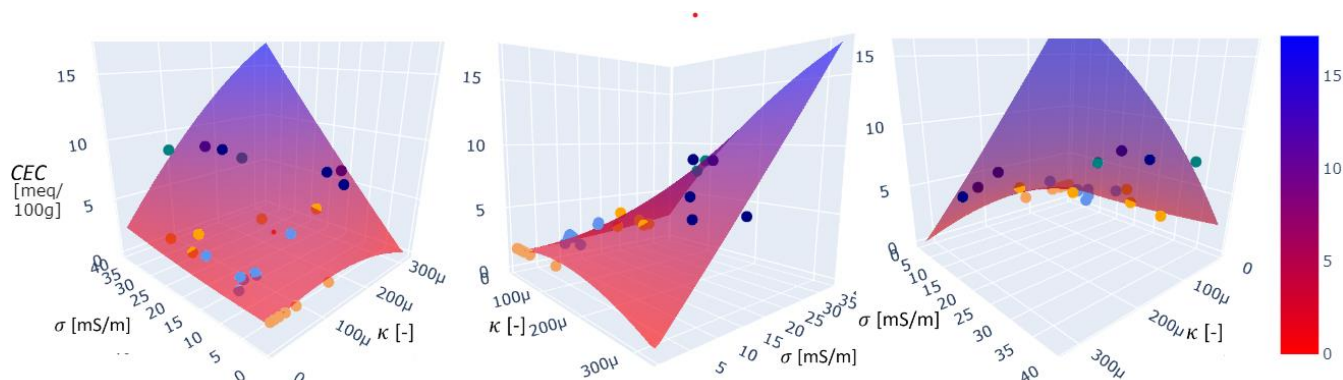
Figure 5 Implemented CEC PTF for sandy samples (clay<16.1) (Equation 2) with a R^2=0.94. The model is colored in vertical axis from red to blue to visualize its shape. Colored dots represent the samples used in the sandy group, belonging to different sites that match the colors in Figure 1.

For clayey samples, σ and *Clay* features resulted in the best performance with a training and testing R^2 equal to 0.89 and 0.82, respectively. This result is in line with the literature since the link between CEC, σ and *Clay* is well documented (Glover, 2015; Wunderlich et al., 2013). For clayey samples, κ was not an outstanding feature, likely due to the influence of larger colloid surface that may not be effectively characterized by κ .

3.3 κ_*- CEC statistics

The partial correlation between κ_* and CEC, while controlling for (removing the effect of) *Clay*, was found to be 0.61 for sandy samples, and -0.14 for clayey samples. This indicates that in sandy samples, κ_* is just partially influenced by *Clay*. For clayey samples, however, κ_* is heavily influenced by the soil's clay content, making the correlation between κ_* and CEC minor if the effect of *Clay* is removed. Consequently, predicting CEC using *Clay* alone is as effective as using both *Clay* and κ_* (median testing R^2 of 0.66 and 0.64, respectively), while κ_* alone is a poor predictor (see Figure 4).

4 Limitations

The main limitations of the analyzed results are related to the dataset size; a larger sample size could improve the robustness of the findings. Additionally, all collected samples come from non-tropical regions, where organic matter content and bacterial activity do not significantly influence soil κ. In contrast, these factors may contribute substantially to higher soil

CEC in other environments (Seybold et al., 2005). Therefore, the results are valid for the sampled sites that belong to European soils, and applications to scenarios beyond this range of soils should be approached with caution. Specifically, the

220   model shown in Equation 2 is valid for samples with clay content between 2.9% to 16.1%, σ between 0.55 mS/m to 39 mS/m, κ_* between 8 to 320 µ, and CEC between 1.6 meq/100g to 8.7 meq/100g.

5 Conclusions

For the first time, the link between soil κ and CEC has been explored using data that extends beyond the site level. By

225   analyzing soil samples across Europe, encompassing a range of diverse soil physicochemical properties, we found that κ_* significantly contributes to predicting soil CEC, particularly in sandy samples, and this contribution is linearly independent of the soil clay content. Conversely, soil κ measured in the laboratory was less effective, likely due to the disturbance of soil structure and soil density.

Based on these findings, we proposed a novel PTF for CEC in sandy samples, with a R^2 of 0.94, based on σ and κ_*, which

230   likely relate to the variable and permanent components of CEC, respectively. This PTF is valuable because both σ and κ_* are quick and inexpensive to measure in the field, making it straightforward to predict CEC under field conditions. For instance, it can be used to quickly assess the fertility of sandy soils across agricultural fields.

Further research, along with expanding the existing database, could enhance CEC modeling and provide deeper insights into the κ_*-CEC relationship. These advances could help integrate independent geophysical properties such as σ and κ, to

235   quantify key soil properties like CEC, advancing a more holistic approach towards soil characterization.

Data availability

10.5281/zenodo.13971643

Code availability

240   https://github.com/orbit-ugent/kappa-CEC

Author contribution

PS, MV and JV designed the surveys and carried them out. MV developed the model code and performed the simulations and contributed to statistical formal analysis along HG. JV, HG, PS and WC gave writing advice. MV prepared the manuscript with contributions from all co-authors.

245

Competing interests

The authors declare that they have no conflict of interest.

250 **Special issue statement**

Agrogeophysics: illuminating soil's hidden dimensions

Acknowledgements

255

References

Ayoubi, S., Mohsen Jabbari, & Hossein Khademi. (2018). Multiple linear modeling between soil properties, magnetic susceptibility and heavy metals in various land uses. *Modeling Earth Systems and Environment (2018) 4:579–589 Https://Doi.Org/10.1007/S40808-018-0442-0*, *4*, 579–589. https://doi.org/10.1007/s40808-018-0442-0

260 Busenberg, E., & Clemency, C. V. (1973). Determination of the Cation Exchange Capacity of Clays and Soils Using an Ammonia Electrode. *Clays and Clay Minerals*, *21*(4), 213–217. https://doi.org/10.1346/CCMN.1973.0210403

Chapman, H. D. (1965). Cation-Exchange Capacity. In A. G. Norman (Ed.), *Agronomy Monographs* (pp. 891–901). American Society of Agronomy, Soil Science Society of America. https://doi.org/10.2134/agronmonogr9.2.c6

Ciesielski, H., Sterckeman, T., Santerne, M., & Willery, J. P. (1997a). A comparison between three methods for the

265   determination of cation exchange capacity and exchangeable cations in soils. *Agronomie*, *17*(1), 9–16. https://doi.org/10.1051/agro:19970102

Ciesielski, H., Sterckeman, T., Santerne, M., & Willery, J. P. (1997b). Determination of cation exchange capacity and exchangeable cations in soils by means of cobalt hexamine trichloride. Effects of experimental conditions. *Agronomie*, *17*(1), 1–7. https://doi.org/10.1051/agro:19970101

270   de Mello, D., Demattê, J. A. M., Silvero, N. E. Q., Di Raimo, L. A. D. L., Poppiel, R. R., Mello, F. A. O., Souza, A. B., Safanelli, J. L., Resende, M. E. B., & Rizzo, R. (2020). Soil magnetic susceptibility and its relationship with naturally occurring processes and soil attributes in pedosphere, in a tropical environment. *Geoderma*, *372*, 114364. https://doi.org/10.1016/j.geoderma.2020.114364

Dearing, J. A. (1994). *Environmental Magnetic Susceptibility. Using the Bartington MS2 system*.

275   Dearing, J. A., Hay, K. L., Baban, S. M. J., Huddleston, A. S., Wellington, E. M. H., & Loveland, P. J. (1996). Magnetic susceptibility of soil: An evaluation of conflicting theories using a national data set. *Geophysical Journal International*, *127*(3), 728–734.

Emamgolizadeh, S., Bateni, S. M., Shahsavani, D., Ashrafi, T., & Ghorbani, H. (2015). Estimation of soil cation exchange capacity using Genetic Expression Programming (GEP) and Multivariate Adaptive Regression Splines (MARS).

280   *Journal of Hydrology*, *529*, 1590–1600. https://doi.org/10.1016/j.jhydrol.2015.08.025

Garré, S., Blanchy, G., Caterina, D., De Smedt, P., Romero-Ruiz, A., & Simon, N. (2022). Geophysical methods for soil applications. In *Reference Module in Earth Systems and Environmental Sciences*. Elsevier. https://doi.org/10.1016/B978-0-12-822974-3.00152-X

Ghorbani, H., Kashi, H., Hafezi Moghadas, N., & Emamgholizadeh, S. (2015). Estimation of Soil Cation Exchange Capacity

285   using Multiple Regression, Artificial Neural Networks, and Adaptive Neuro-fuzzy Inference System Models in Golestan Province, Iran. *Communications in Soil Science and Plant Analysis*, *46*(6), 763–780. https://doi.org/10.1080/00103624.2015.1006367

Glover, P. W. J. (2015). Geophysical Properties of the Near Surface Earth: Electrical Properties. In *Treatise on Geophysics* (pp. 89–137). Elsevier. https://doi.org/10.1016/B978-0-444-53802-4.00189-5

290   Jordanova, N. (2017). *Soil Magnetism. Applications in Pedology, Environmental Science and Agriculture*. Academic Press.

Khaledian, Y., Brevik, E. C., Pereira, P., Cerdà, A., Fattah, M. A., & Tazikeh, H. (2017). Modeling soil cation exchange capacity in multiple countries. *CATENA*, *158*, 194–200. https://doi.org/10.1016/j.catena.2017.07.002

Logsdon, S. D., Green, T. R., Seyfried, M., Evett, S. R., & Bonta, J. (2010). Hydra Probe and Twelve-Wire Probe Comparisons in Fluids and Soil Cores. *Soil Science Society of America Journal*, *74*(1), 5–12.

295   https://doi.org/10.2136/sssaj2009.0189

Maher, B. A. (1998). Magnetic properties of modern soils and Quaternary loessic paleosols: Paleoclimatic implications. *Palaeogeogr Palaeoclimatol Palaeoecol*, *137*(1–2), 25–54.

Maier, G., Scholger, R., & Schön, J. (2006). The influence of soil moisture on magnetic susceptibility measurements. *Journal of Applied Geophysics*, *59*(2), 162–175.

300   McLachlan, P., Schmutz, M., Cavailhes, J., & Hubbard, S. S. (2022). Estimating grapevine-relevant physicochemical soil zones using apparent electrical conductivity and in-phase data from EMI methods. *Geoderma*, *426*, 116033. https://doi.org/10.1016/j.geoderma.2022.116033

Mendoza Veirana. (2024). *orbit-ugent/kappa-CEC: First release* (Version 0.1) [Computer software]. Zenodo. https://doi.org/10.5281/ZENODO.13970660

305   Mendoza Veirana, G., Verhegge, J., Cornelis, W., & De Smedt, P. (2023). Soil dielectric permittivity modelling for 50 MHz instrumentation. *Geoderma*, *438*, 116624. https://doi.org/10.1016/j.geoderma.2023.116624

Miller, W. F. (1970). Inter-regional predictability of cation-exchange capacity by multiple regression. *Plant and Soil*, *33*(1–3), 721–725. https://doi.org/10.1007/BF01378263

Poggio, L., De Sousa, L. M., Batjes, N. H., Heuvelink, G. B. M., Kempen, B., Ribeiro, E., & Rossiter, D. (2021). SoilGrids

310   2.0: Producing soil information for the globe with quantified spatial uncertainty. *SOIL*, *7*(1), 217–240. https://doi.org/10.5194/soil-7-217-2021

Romero-Ruiz, A., Linde, N., Keller, T., & Or, D. (2018). A Review of Geophysical Methods for Soil Structure Characterization: Geophysics and soil structure. *Reviews of Geophysics*, *56*(4), 672–697. https://doi.org/10.1029/2018RG000611

315   Seybold, C. A., Grossman, R. B., & Reinsch, T. G. (2005). Predicting Cation Exchange Capacity for Soil Survey Using Linear Models. *Soil Science Society of America Journal*, *69*(3), 856–863. https://doi.org/10.2136/sssaj2004.0026

Siqueira, D. S., Marques Jr, J., Matias, S. S. R., Barrón, V., Torrent, J., Baffa, O., & Oliveira, L. C. (2010). Correlation of properties of Brazilian Haplustalfs with magnetic susceptibility measurements: Magnetic susceptibility in Brazilian Haplustalfs. *Soil Use and Management*, *26*(4), 425–431. https://doi.org/10.1111/j.1475-2743.2010.00294.x

320   Sumner, M. E., & Miller, W. P. (2018). Cation Exchange Capacity and Exchange Coefficients. In D. L. Sparks, A. L. Page, P. A. Helmke, R. H. Loeppert, P. N. Soltanpour, M. A. Tabatabai, C. T. Johnston, & M. E. Sumner (Eds.), *SSSA Book Series* (pp. 1201–1229). Soil Science Society of America, American Society of Agronomy. https://doi.org/10.2136/sssabookser5.3.c40

Van Looy, K., Bouma, J., Herbst, M., Koestel, J., Minasny, B., Mishra, U., Montzka, C., Nemes, A., Pachepsky, Y. A.,
325   Padarian, J., Schaap, M. G., Tóth, B., Verhoef, A., Vanderborght, J., van der Ploeg, M. J., Weihermüller, L., Zacharias, S., Zhang, Y., & Vereecken, H. (2017). Pedotransfer Functions in Earth System Science: Challenges and Perspectives. *Reviews of Geophysics*, *55*(4), 1199–1256. https://doi.org/10.1002/2017RG000581

Verhegge, J., Mendoza Veirana, G., Cornelis, W., Crombé, P., Grison, H., De Kort, J.-W., Rensink, E., & De Smedt, P. (2021). Working the land, searching the soil: Developing a geophysical framework for Neolithic land-use studies.
330   Project introduction,-methodology, and preliminary results at 'Valther Tweeling.' *Notae Praehistoricae*, *41*, 187–197.

Wunderlich, T., Petersen, H., Hagrey, S. A. al, & Rabbel, W. (2013). Pedophysical Models for Resistivity and Permittivity of Partially Water-Saturated Soils. *Vadose Zone Journal*, *12*(4), vzj2013.01.0023. https://doi.org/10.2136/vzj2013.01.0023

335   ZH instruments. (2022). *Magnetic susceptibility meter SM-30. User's manual.* http://www.zhinstruments.com/assets/sm-30-manual.pdf